Hydrocarbon Processing

International Edition: DOI: 10.1002/anie.201510599
German Edition: DOI: 10.1002/ange.201510599

Facile Preparation of Ni_2P with a Sulfur-Containing Surface Layer by Low-Temperature Reduction of $Ni_2P_2S_6$

Song Tian, Xiang Li, Anjie Wang, Roel Prins, Yongying Chen, and Yongkang Hu*

Abstract: *Preparation of Ni_2P by temperature-programmed reduction (TPR) of a phosphate precursor is challenging because the P–O bond is strong. An alternative approach to synthesizing Ni_2P, by reduction of nickel hexathiodiphosphate ($Ni_2P_2S_6$), is presented. Conversion of $Ni_2P_2S_6$ into Ni_2P occurs at 200–220 °C, a temperature much lower than that required by the conventional TPR method (typically 500 °C). A sulfur-containing layer with a thickness of about 4.7 nm, composed of tiny crystallites, was observed at the surface of the obtained Ni_2P catalyst (Ni_2P–S). This is a direct observation of the sulfur-containing layer of Ni_2P, or the so-called nickel phosphosulfide phase. Both the hydrodesulfurization activity and the selective hydrogenation performance of Ni_2P-S were superior to that of the catalyst prepared by the TPR method, suggesting a positive role of sulfur on the surface of Ni_2P-S. These features render Ni_2P-S a legitimate alternative non-precious metal catalyst for hydrogenation reactions.*

Phosphorus reacts with most elements of the periodic table to form a diverse class of compounds known as phosphides.[1] Many metal phosphides accept several stoichiometries, providing a large number of structures.[2] According to the metal/phosphorus ratio (M:P), the transition-metal phosphides (TMPs) can be classified as metal-rich phosphides (M:P > 1), monophosphides (M:P = 1), and phosphorus-rich phosphides (M:P < 1). Phosphorus-rich TMPs are semiconducting and are considerably less stable than metal-rich compounds.[3] Metal-rich TMPs are covalent compounds and usually possess metallic character.[3] They are hard, electrical conductors, and have high thermal stabilities and resistance to chemical attack, and thus attract much attention as catalytic materials for hydrogenation reactions.[3]

As early as the 1950s, the metal-rich dinickel phosphide, $NiP_{0.584}$, was reported to be active in vapor-phase reduction of nitrobenzene with hydrogen into aniline and water.[4] Thereafter, the hydrogenation, dimerization, polymerization, and hydroformylation–carbonylation performance of TMPs were examined in the 1970s and 1980s.[5] They were found to possess lower hydrogenation activity than their metallic counterparts.[5] It was not until 1996, when Robinson et al.[6] reported that Ni_2P had higher activity in quinoline hydrodenitrogenation (HDN) than a commercial sulfided Ni-Mo/Al_2O_3 catalyst, that they again caught the attention of the scientific community as a new family of hydrotreating catalysts. Among the investigated TMPs (Fe_2P, CoP, MoP, WP, and Ni_2P for example), Ni_2P is the most active catalyst in the simultaneous hydrodesulfurization (HDS) of dibenzothiophene (DBT) and HDN of quinoline.[7] In recent years, TMPs have been reported as promising for many other reactions; such as hydrodeoxygenation, hydrogen evolution, and selective hydrogenation.[8]

There are various methods for synthesizing TMPs, of which the most commonly used is the temperature-programmed reduction of metal phosphate precursors in flowing H_2 at elevated temperature (TPR).[9] The P–O bond in phosphate is strong, therefore its reduction requires high temperatures (generally > 500 °C).[9] One approach to achieve lowering of the reduction temperature is to use phosphorus sources other than phosphate (for example, dihydrogenphosphite,[10] hypophosphite,[11] PH_3,[12] tris(trimethylsilyl)phosphine, or trioctylphosphine[13]); or to perform the solvothermal reduction with Na_3P or phosphorus (yellow or red).[9] However, according to Da Silva et al.[14] and Wang et al.,[15] these methods present disadvantages that may limit their application. Another alternative is to use precursors containing P–S bonds, which are easier to break than P–O bonds.[16] In 1996, two years before the TPR method was employed by Li et al. for the synthesis of TMPs,[17] Robinson et al. obtained a sulfur-free Ni_2P catalyst by decomposing a nickel thiophosphate precursor (denoted by the authors as $NiPS_3$) under a 10 vol% H_2S/H_2 atmosphere.[6] Nevertheless, the $NiPS_3$ precursor was synthesized in this study by reacting stoichiometric quantities of elementary nickel, red phosphorus, and sulfur at high temperature (700 °C) and over a long reaction period (3.5 days). By adopting a soft-chemistry route, $NiPS_3$ can be synthesized by reaction of $NiCl_2$ or $Ni(NO_3)_2$ with Li_2PS_3 at room temperature.[16]

One of the unique properties of TMPs relative to their metallic counterparts is that sulfur plays a positive role in some reactions performed over TMPs. For both Ni_2P and MoP, the most active HDS site has been identified as a surface phosphosulfide that is generated during reaction.[18] Kibsgaard and Jaramillo found that introduction of sulfur onto the surface of MoP produced a molybdenum phosphosulfide catalyst with superb activity and stability for hydrogen evolution in acidic environments.[19] The surface sulfidation of Ni_2P is more difficult than that for MoP. Sun et al. demonstrated that MoP/SiO_2 can be sulfided with a mixture of thiophene/H_2, whereas more severe sulfiding conditions

[*] S. Tian, Dr. X. Li, Prof. Dr. A. Wang, Y. Chen, Prof. Y. Hu
State Key Laboratory of Fine Chemicals, School of Chemical Engineering, Dalian University of Technology
No. 2 Linggong Road, Dalian 116024 (P.R. China)
E-mail: lixiang@dlut.edu.cn
Prof. Dr. R. Prins
Institut für Chemie- und Bio-Ingenieurwissenschaften, ETH Zürich
Vladimir-Prelog-Weg 1-5/10, 8093 Zürich (Switzerland)

Supporting information for this article can be found under http://dx.doi.org/10.1002/anie.201510599.

and an H_2S/H_2 mixture were required to transform Ni_2P/SiO_2 into its phosphosulfide counterpart.[20]

Herein, we report the preparation of Ni_2P by reduction of nickel hexathiodiphosphate ($Ni_2P_2S_6$) at a temperature as low as 220 °C. $Ni_2P_2S_6$ was obtained at room temperature from the solid reaction of $NiCl_2$ and $Na_4P_2S_6$. A distinct sulfur-containing layer was observed at the surface of the derived Ni_2P catalyst, which might explain its high HDS and selective hydrogenation performances in comparison with those of the Ni_2P catalyst prepared by the conventional TPR method.

$Ni_2P_2S_6$ was first synthesized by reacting $NiCl_2$ with $Na_4P_2S_6$, a product of the reaction of Na_2S and PCl_3.[21] In the XRD pattern of the sample (Supporting Information, Figure S1), the ratio of the intensity of the peak at $2\theta = 36.2°$ relative to the peak at $2\theta = 14.0°$, and particularly the presence of a peak at $2\theta = 45.7°$, indicate that the major phase in the sample was $Ni_2P_2S_6$ (PDF card 33-0952) rather than the $NiPS_3$ precursor (PDF card 78-0499) described in a previous study.[16] A small amount of impurity, probably NiS (PDF card 65-3419), was also detected.

$Ni_2P_2S_6$ was treated in a tubular reactor under a H_2 or Ar flow for 2 h, at temperatures ranging from 200–300 °C, and a pressure of 1.0 MPa. Figure 1 shows the development of the

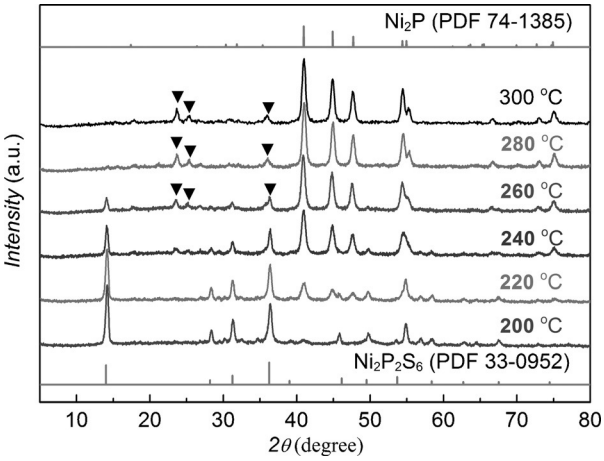

Figure 1. Evolution of the XRD patterns of $Ni_2P_2S_6$ during reduction into Ni_2P in a H_2 flow (1.0 MPa and a H_2 flow rate of 100 mL min^{-1}). ▼ = impurity.

XRD pattern of the $Ni_2P_2S_6$ sample after H_2 treatment (1.0 MPa H_2 at a 100 mL min^{-1} flow rate) over an increasing temperature range. At 200 °C new peaks with very low intensities were detected at 40.7° and 55.0°, respectively, corresponding to the (111) and (211) reflections of the Ni_2P phase (PDF card 74-1385). At 220 °C a mixture of $Ni_2P_2S_6$ and Ni_2P was obtained. Above 260 °C Ni_2P became the dominant phase. Some weak impurity peaks were also present in the XRD pattern above 240 °C. The nature of the impurity cannot be determined on the basis of the present data, and might be phosphate, phosphorus sulfide, sulfur, or a mixture of these compounds. Further research is needed to determine the nature of the unknown impurity.

In Ar atmosphere (1.0 MPa and 100 mL min^{-1}), no Ni_2P was formed under the temperatures investigated. Moreover, the peak at $2\theta = 14.0°$ became the most intense diffraction line (Supporting Information, Figure S2), suggesting that some of the $Ni_2P_2S_6$ species was converted to $NiPS_3$. Apparently, conversion of $Ni_2P_2S_6$ into Ni_2P is a result of reduction of $Ni_2P_2S_6$ in H_2 rather than thermal decomposition. Reduction of $Ni_2P_2S_6$ starts at a temperature between 200 and 220 °C, much lower than that required by the conventional TPR method (typically 500 °C), but also lower than that reported for the conversion of $NiPS_3$ into Ni_2P. Because of the slow kinetics of reduction, $Ni_2P_2S_6$ was reduced to Ni_2P after 8 h at 220 °C (Supporting Information, Figure S3). By means of in situ XRD and EXAFS, Loboué et al. observed that Ni_2P can be obtained from a $NiPS_3$ sample prepared by a soft-chemistry approach at a reduction temperature of 300 °C, whereas a well-crystallized $NiPS_3$ precursor (PDF card 78-0499) was first reduced into a Ni_5P_4 intermediate at 350 °C, with Ni_2P formation at 500 °C.[16] Besides temperature, H_2 pressure is another determining factor in the reduction of $Ni_2P_2S_6$ into Ni_2P. At 0.1 MPa H_2 pressure, no Ni_2P was formed at temperatures up to 300 °C after an 8 h reduction of $Ni_2P_2S_6$ (Supporting Information, Figure S4). H_2 flow rate is not as important for reduction as temperature and H_2 pressure. At 1.0 MPa H_2 pressure and 300 °C, a decrease of H_2 flow rate from 100–25 mL min^{-1} did not affect the formation of Ni_2P (Supporting Information, Figure S5).

The XPS spectra of Ni_2P samples prepared by the conventional TPR method (Ni_2P-TPR), and the reduction of $Ni_2P_2S_6$ at 300 °C with 1.0 MPa H_2 at a flow rate of 100 mL min^{-1} for 2 h (Ni_2P-S), are illustrated in Figure 2. Two broad peaks were observed in the Ni 2p spectrum of Ni_2P-TPR. The major peak at approximately 852.1 eV is related to reduced $Ni^{\delta+}$ ($0 < \delta < 2$) in Ni_2P, while the other peak at about 855.5 eV corresponds to Ni^{2+}.[22] In the P 2p spectrum of Ni_2P-TPR, the doublet at 129.4 and 130.2 eV can be assigned to P bonded to Ni in the form of a phosphide, whereas the most intense peak at 133.8 eV indicates a surface PO_4^{3-} species.[19] The presence of Ni^{2+} and PO_4^{3-} species must result from air exposure of the sample before XPS measurement. In the case of Ni_2P-S, Ni^{2+} became the predominant Ni species. Shifting of the major P 2p peak to 135.1 eV arises from P_2O_5.[23] Apparently, the surface oxidation behavior of Ni_2P-S is

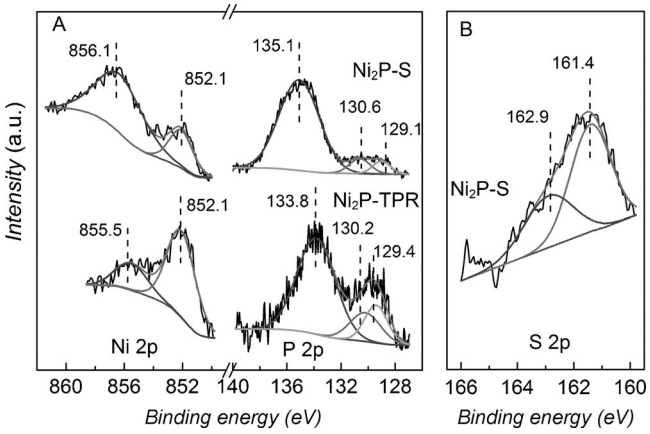

Figure 2. XPS spectra of Ni_2P-TPR and Ni_2P-S in the A) Ni 2p and P 2p regions, and B) S 2p region.

different from that of Ni_2P-TPR upon exposure to air. Ni_2P-S is easier to oxidize than Ni_2P-TPR, as discussed below. Sulfur was only detected in Ni_2P-S. The surface S:Ni ratio determined by XPS was 0.41, which was 5.6 times larger than that measured by XRF (0.073), suggesting that sulfur is enriched in the surface of Ni_2P-S. The S 2p peak (Figure 2B) can be deconvoluted into two Gaussian peaks, located at 161.4 and 162.9 eV, assigned to sulfide species (S^{2-}) and thiolate-type sulfur, respectively.[18b] These sulfur species are similar to those observed in the so-called "phosphosulfide" phase.[18b] Ni_2P-TPR demonstrated a CO uptake of 4.7 $\mu mol\,g^{-1}$, whereas that of Ni_2P-S was almost zero. It seems that the presence of sulfur on the surface of Ni_2P-S blocks the adsorption of CO.

TEM images demonstrate that particles of Ni_2P-TPR were heterogeneously distributed with an average particle size of 304 nm, which was much larger than that for Ni_2P-S (100 nm; Supporting Information, Figure S6). This might be a result of the low temperature (300 °C) employed during reduction of $Ni_2P_2S_6$ into Ni_2P. At higher resolution (Figure 3), lattice fringes were clearly seen in TEM images of both samples with an interplane distance of 0.22 nm corresponding to the (111) plane of Ni_2P, confirming the formation of the Ni_2P phase. However, the surface of Ni_2P-S was quite different from that of Ni_2P-TPR. An amorphous layer with a thickness of approximately 1.5 nm, resulting from O_2 passivation, was observed at the surface of the Ni_2P-TPR particles, which is in agreement with the MoP passivation layer reported in our previous study.[24] On the other hand, Ni_2P-S particles were surrounded by a thick layer (about 4.7 nm) composed of tiny crystallites. The lattice spacing in the (111) plane of some surface crystallites was measured as 0.24 nm. This value is slightly larger than that for the bulk (0.22 nm), which suggests incorporation of sulfur originating from H_2S released during $Ni_2P_2S_6$ reduction. This theory is supported by an absence of sulfur in the bulk phase. Assuming that all the sulfur species are located in the thick surface layer with a S:Ni ratio of 0.41 (determined by XPS), and that Ni species are uniformly distributed in Ni_2P-S, and considering the thickness of the layer (4.7 nm), as well as the average crystallite size of Ni_2P-S (100 nm), the S:Ni ratio in Ni_2P-S is estimated to be 0.10. This value is close to that measured by XRF (0.073). In fact, the surface S:Ni ratio (0.41) is only slightly higher than that of a stable nickel phosphosulfide phase (Ni_3PS, 0.33) predicted by density functional theory calculations.[25] The combined results suggest that reduction of $Ni_2P_2S_6$ creates a phosphosulfide phase at the surface, leaving the bulk of the catalyst almost intact as Ni_2P.

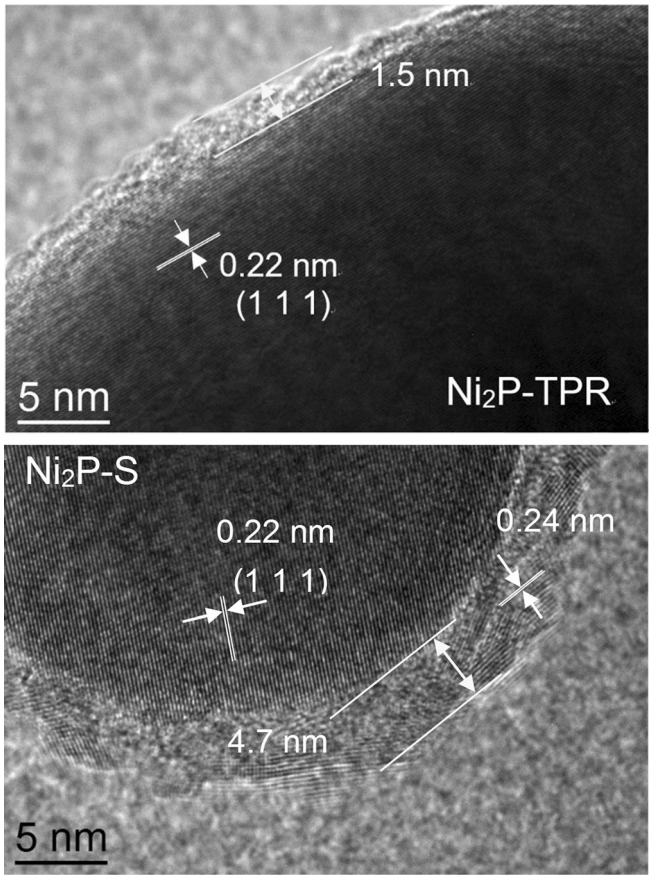

Figure 3. TEM images of Ni_2P-TPR and Ni_2P-S.

Different surface structures are likely to be responsible for the differing surface oxidation behaviors of Ni_2P-TPR and Ni_2P-S, revealed by XPS (Figure 2). Based on the study of Pakes et al. regarding anodic film growth on InP,[23a] we propose that the surface phosphorus species of Ni_2P-TPR are immobile. Outward migration of Ni species leads to formation of Ni oxide, while inward migration of oxygen yields PO_4^{3-} species at the interphase (Supporting Information, Scheme S1). For Ni_2P-S, tiny crystallites at the surface may react with oxygen much more vigorously than the surface of bulk Ni_2P-TPR particles, leading to the formation of Ni oxide and P_2O_5. However, it is still not possible to separate these surface phases. Further experimental and theoretical work is needed to fully understand their nature.

The HDS performance of Ni_2P-S and Ni_2P-TPR were evaluated using DBT as a sulfur-containing molecule. DBT undergoes HDS by two parallel pathways (Supporting Information, Scheme S2): direct desulfurization (DDS), and hydrogenation (HYD). DDS leads to formation of biphenyl (BP), while HYD yields mainly cyclohexylbenzene (CHB) and dicyclohexane. Because the hydrogenation of BP to CHB is negligible in the presence of DBT, BP selectivity (S_{BP}) is used as a measure of the DDS pathway, while (1-S_{BP}) represents the HYD pathway. The conversion of DBT over Ni_2P-S was two times greater than that over Ni_2P-TPR (Table 1). Such a significant increase in the HDS activity of Ni_2P-S cannot only be attributed to a decrease in particle size, because Ni_2P-S and Ni_2P-TPR demonstrated different reaction pathway selectivities for the HDS of DBT. Moreover, it has been determined by Oyama et al.[26] that the HDS of DBT over Ni_2P is a structure insensitive reaction. The HYD pathway selectivity of Ni_2P-S was 8% higher than that of Ni_2P-TPR (Table 1), indicating that the HYD pathway is enhanced relative to DDS after formation of the sulfur-containing layer.

The low HDS reactivity of DBT and its alkylated derivatives is usually attributed to a steric hindrance effect that prevents adsorption of sulfur atoms on the catalytic site.

Table 1: The catalytic performances of Ni_2P-TPR and Ni_2P-S: HDS of DBT, and selective hydrogenation of phenylacetylene, naphthalene, nitrobenzene, and *p*-chloronitrobenzene.

Reaction	Conversion [%]		Selectivity [%]	
	Ni_2P-S	Ni_2P-TPR	Ni_2P-S	Ni_2P-TPR
HDS of DBT	50.2	24.8	33.5[a]	26.1[a]
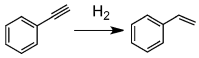	90.2	10.1	95.6	89.2
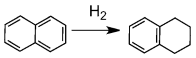	85.4	51.2	99.7	95.4
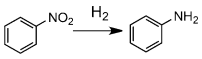	84.2	65.4	99.2	95.3
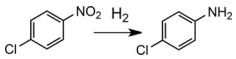	43.3	18.7	95.7	94.4

[a] HYD pathway selectivity, $(1-S_{BP})\times 100\%$.

Hydrogenation of the aromatic ring, which removes steric hindrance, remarkably enhances the HDS reactivity of these refractory polyaromatic sulfur-containing compounds. Our previous work,[8c] and that of Carenco et al.,[8d] has demonstrated that Ni_2P is promising for the chemoselective hydrogenation of alkynes. Therefore, we further studied the selective hydrogenation of phenylacetylene, naphthalene, nitrobenzene, and *p*-chloronitrobenzene over Ni_2P-S and Ni_2P-TPR. The results are listed in Table 1. The two catalysts exhibited high selectivities ($\geq 89\%$) toward partially hydrogenated products. For all reactions a significant increase was observed in the activity of Ni_2P-S relative to Ni_2P-TPR, as well as a minor increase in product selectivities. For instance, conversion of styrene over Ni_2P-S was 90%, 9 times higher than that over Ni_2P-TPR. The conversion of *p*-chloronitrobenzene increased from 18% over Ni_2P-TPR to 43% over Ni_2P-S without facilitating the dechlorination reaction, because selectivity for *p*-chloroaniline was equally high over both catalysts (about 95%). The above features and a facile preparative route suggest that Ni_2P-S is a legitimate alternative to non-precious metal catalysts, such as Ni_2P-TPR, in selective hydrogenation reactions.

In summary, reduction of $Ni_2P_2S_6$ is a facile and promising method for preparation of Ni_2P. Conversion of $Ni_2P_2S_6$ into Ni_2P occurs at temperatures as low as 200–220 °C and at 1.0 MPa H_2 pressure. A distinct sulfur-containing layer with a thickness of about 4.7 nm, composed of tiny crystallites, was observed at the surface of the obtained Ni_2P catalyst. This is a direct observation of the sulfur-containing layer of Ni_2P, or the so-called nickel phosphosulfide phase. Sulfur occurred as a mixture of S^{2-} and thiolate species. Both the HDS activity and selective hydrogenation performance of Ni_2P-S were superior to that of Ni_2P-TPR, suggesting a positive role of the surface sulfur species in catalytic processes.

Experimental Section

$Na_4P_2S_6{\cdot}6H_2O$ was synthesized by reacting Na_2S with PCl_3 following a method described elsewhere.[21] Prepared $Na_4P_2S_6{\cdot}6H_2O$ (1.80 g) was then mixed with $NiCl_2{\cdot}6H_2O$ (1.88 g) at a molar ratio of 1:2 and manually ground in a mortar for 30 min. The resulting mixture was sealed in a quartz tube under vacuum (1.3×10^{-2} Pa N_2) and heated at 500 °C for 24 h. The solid product was thoroughly washed with water and ethanol to remove NaCl. After drying at 120 °C for 6 h a black powder of $Ni_2P_2S_6$ was obtained. The phosphate precursor of Ni_2P-TPR was prepared by a co-precipitation method. An aqueous solution of $(NH_4)_2HPO_4$ (1.77 g) in deionized water (10 mL) was added dropwise to a solution of $Ni(NO_3)_2{\cdot}6H_2O$ (3.90 g) in deionized water (15 mL) with stirring. The resulting precipitate was stirred while the water was evaporated to obtain a solid product, which was dried at 120 °C for 12 h and calcined at 500 °C for 6 h to obtain the final oxidic precursor with a Ni:P molar ratio of 1. This value is exactly the same as that of $Ni_2P_2S_6$. Further details regarding preparation of Ni_2P, characterization techniques, as well as hydrodesulfurization and hydrogenation reactions are summarized in the Supporting Information.

Acknowledgements

This work was financially supported by the Natural Science Foundation of China (21173033, U1162203, and 21473017), the Fundamental Research Funds for the Central Universities (DUT13LK18), the PetroChina Innovation Foundation (2014D-5006-0402), the State Key Laboratory of Fine Chemicals (KF1306), and the Scientific Research Fund of Liaoning Provincial Education Department (L2013023).

Keywords: hydrodesulfurization · nickel phosphides · selective hydrogenation · sulfur-containing layer

How to cite: *Angew. Chem. Int. Ed.* **2016**, *55*, 4030–4034
Angew. Chem. **2016**, *128*, 4098–4102

[1] S. T. Oyama, *J. Catal.* **2003**, *216*, 343–352.
[2] S. Carenco, D. Portehault, C. Boissière, N. Mézailles, C. Sanchez, *Chem. Rev.* **2013**, *113*, 7981–8065.
[3] S. T. Oyama, T. Gott, H. Zhao, Y.-K. Lee, *Catal. Today* **2009**, *143*, 94–107.
[4] N. P. Sweeny, C. S. Rohrer, O. W. Brown, *J. Am. Chem. Soc.* **1958**, *80*, 799–800.
[5] a) E. L. Muetterties, J. C. Sauer, *J. Am. Chem. Soc.* **1974**, *96*, 3410–3415; b) F. Nozaki, R. Adachi, *J. Catal.* **1975**, *40*, 166–172.
[6] W. R. A. M. Robinson, J. N. M. van Gastel, T. I. Korányi, S. Eijsbouts, J. A. R. van Veen, V. H. J. de Beer, *J. Catal.* **1996**, *161*, 539–550.
[7] H. Zhao, S. T. Oyama, H.-J. Freund, R. Wlodarczyk, M. Sierka, *Appl. Catal. B* **2015**, *164*, 204–216.
[8] a) A. Cho, H. Kim, A. Iino, A. Takagaki, S. T. Oyama, *J. Catal.* **2014**, *318*, 151–161; b) E. J. Popczun, J. R. McKone, C. G. Read, A. J. Biacchi, A. M. Wiltrout, N. S. Lewis, R. E. Schaak, *J. Am. Chem. Soc.* **2013**, *135*, 9267–9270; c) X. Li, Y. Zhang, A. Wang, Y. Wang, Y. Hu, *Catal. Commun.* **2010**, *11*, 1129–1132; d) S. Carenco, A. Leyva-Pérez, P. Concepción, C. Boissière, N. Mézailles, C. Sanchez, A. Corma, *Nano Today* **2012**, *7*, 21–28.
[9] R. Prins, M. E. Bussell, *Catal. Lett.* **2012**, *142*, 1413–1436.
[10] J. A. Cecilia, A. Infantes-Molina, E. Rodríguez-Castellón, A. Jiménez-López, *J. Catal.* **2009**, *263*, 4–15.
[11] Q. Guan, W. Li, M. Zhang, K. Tao, *J. Catal.* **2009**, *263*, 1–3.
[12] S. Yang, R. Prins, *Chem. Commun.* **2005**, 4178–4180.
[13] K.-S. Cho, H.-R. Seo, Y.-K. Lee, *Catal. Commun.* **2011**, *12*, 470–474.
[14] V. T. da Silva, L. A. Sousa, R. M. Amorim, L. Andrini, S. J. A. Figueroa, F. G. Requejo, F. C. Vicentini, *J. Catal.* **2011**, *279*, 88–102.

[15] A. Wang, M. L. Qin, J. Guan, L. Wang, H. C. Guo, X. Li, Y. Wang, R. Prins, Y. K. Hu, *Angew. Chem. Int. Ed.* **2008**, *47*, 6052–6054; *Angew. Chem.* **2008**, *120*, 6141–6143.
[16] H. Loboué, C. Guillot-Deudon, A. F. Popa, A. Lafond, B. Rebours, C. Pichon, T. Cseri, G. Berhault, C. Geantet, *Catal. Today* **2008**, *130*, 63–68.
[17] W. Li, B. Dhandapani, S. T. Oyama, *Chem. Lett.* **1998**, *27*, 207–208.
[18] a) T. Kawai, K. K. Bando, Y.-K. Lee, S. T. Oyama, W. J. Chun, K. Asakura, *J. Catal.* **2006**, *241*, 20–24; b) J. Bai, X. Li, A. Wang, R. Prins, Y. Wang, *J. Catal.* **2012**, *287*, 161–169.
[19] J. Kibsgaard, T. F. Jaramillo, *Angew. Chem. Int. Ed.* **2014**, *53*, 14433–14437; *Angew. Chem.* **2014**, *126*, 14661–14665.
[20] F. Sun, W. Wu, Z. Wu, J. Guo, Z. Wei, Y. Yang, Z. Jiang, F. Tian, C. Li, *J. Catal.* **2004**, *228*, 298–310.
[21] T. Fincher, G. LeBret, D. A. Cleary, *J. Solid State Chem.* **1998**, *141*, 274–281.
[22] a) S. J. Sawhill, K. A. Layman, D. R. van Wyk, M. H. Engelhard, C. Wang, M. E. Bussell, *J. Catal.* **2005**, *231*, 300–313; b) I. I. Abu, K. J. Smith, *J. Catal.* **2006**, *241*, 356–366.
[23] a) A. Pakes, P. Skeldon, G. E. Thompson, S. Moisa, G. I. Sproule, M. J. Graham, *Corros. Sci.* **2002**, *44*, 2161–2170; b) H. Zhu, S. McDonnell, X. Qin, A. Azcatl, L. Cheng, R. Addou, J. Kim, P. D. Ye, R. M. Wallace, *ACS Appl. Mater. Interfaces* **2015**, *7*, 13038–13043.
[24] X. Duan, Y. Teng, A. Wang, V. M. Kogan, X. Li, Y. Wang, *J. Catal.* **2009**, *261*, 232–240.
[25] A. E. Nelson, M. Sun, A. S. M. Junaid, *J. Catal.* **2006**, *241*, 180–188.
[26] S. T. Oyama, X. Wang, Y.-K. Lee, K. Bando, F. G. Requejo, *J. Catal.* **2002**, *210*, 207–217.

Received: November 16, 2015
Revised: January 20, 2016
Published online: February 17, 2016

